# Excitation of two interacting electrons as a plasmon-decay mechanism in proton-aluminum collisions

G. A. Bocan and J. E. Miraglia

*Instituto de Astronomía y Física del Espacio, Consejo Nacional de Investigaciones Científicas y Técnicas, Departamento de Física,*
*Facultad de Ciencias Exactas y Naturales, Universidad de Buenos Aires, C.C. 67, Suc. 28, 1428 Buenos Aires, Argentina*
(Received 3 September 2003; published 12 January 2004)

Projectile-induced plasmon excitation in an electron gas has been studied by several authors who proposed two possible mechanisms for these plasmons to decay. In a previous work we considered one of these mechanisms in which the plasmon transfers its energy to a nearly free electron that makes an interband transition. In this paper, the other mechanism is analyzed. A simple model is developed to describe plasmon decay in aluminum via the excitation of two interacting electrons. Results for the transition probability and the excitation power are presented. When contributions from both mechanisms are considered, they account for more than 60% of the excited plasmons. Also, the slope of the plasmon excitation curve is correctly reproduced. The study of first and second differential spectra in angle and energy show that plasmon decay into two interacting electrons is the main source of low-energy electrons moving in the forward direction (with respect to the projectile initial velocity).

## I. INTRODUCTION

Collective excitations that occur in a degenerate electron gas, due to the long range of Coulomb interactions, are usually referred to as plasmons. In the late 1950s both DuBois [1,2] and Nozières and Pines [3] developed formalisms to describe these systems and found that, to the lowest perturbative order [random-phase approximation (RPA) in a free-electron gas model], there was no available mechanism for these plasmons to decay. However, DuBois suggested that, for the electron densities found in metals, interactions beyond the RPA were important and gave the lowest-order contribution to the plasmon damping. That is, a plasmon excited in the bulk could decay by transferring its energy to two, or more, interacting electrons. Alternatively, Nozières and Pines suggested that, in a solid and under the influence of a periodic potential due to the ion cores, plasmons would be damped even in the RPA since there existed some interband transitions at the plasmon energy. Also, they estimated, on heuristic grounds, that the two-electron contribution to the plasmon damping would be proportional to the square of the plasmon wave vector $k^2$.

Early evidence was brought up by DuBois and Kivelson [4] about the failure of two-electron processes to explain available experimental results. They had taken the two-electron contribution to the plasmon damping and performed some calculations of the $k^2$ coefficient including screening effects. Their estimation turned out to be an order of magnitude below experimental values for Al. Also, they mentioned that two-electron processes failed to explain the finite plasmon damping for $k \rightarrow 0$.

The first quantitative description of plasmon decay via interband transitions is due to Chung and Everhart [5], who demonstrated that this mechanism represented an important source of low-energy secondary electrons in nearly free-electron metals. Their work was continued by Rösler and collaborators [6–9] who, in a series of publications, developed most of the theory presently available on the subject.

The first attempt, to our knowledge, to include both two-electron processes and interband transitions in a plasmon linewidth calculation is due to Sturm and Oliveira [10], who obtained that interband transitions were the dominant plasmon-decay mechanism. Later experimental data by Platzman [11] confirmed the existence of strong non-RPA-like correlations in an electron liquid where band-structure effects are unimportant. This brought interest in two-electron contributions to the plasmon damping back to life as can be seen in a couple of publications by Bachlechner and collaborators [12,13].

In a previous work [14], henceforth referred to as I, we developed a simple model to calculate the transition probability and the stopping power for projectile-induced plasmon creation and later decay via the excitation of a nearly free electron. First and second differential spectra in both angle and energy were reported discriminating contributions due to different lattice momenta.

In this paper, we develop a formalism (analogous to the one used in I) to include two-electron contributions to our model and results. As will be shown, they turn out to be important to correctly reproduce the plasmon creation curve slopes at high projectile velocities. Also, we find that this plasmon-decay mechanism is the main source of low-energy electrons in the forward direction (with respect to the projectile initial velocity).

There is a third possible mechanism for plasmon decay that deserves some consideration. The excited plasmon could transfer its energy to a single electron and a phonon (phonon-assisted electron excitation). Sturm and Oliveira considered this possibility and found that for metals such as Li, Na, and K this process represented just a minor contribution to the plasmon linewidth. Based on their result, we will not include this plasmon-decay mechanism in the present paper.

It is important to mention that plasmon creation occurs not only in metals but also in semiconductors and insulators. In these latter cases both the plasmon creation probability

and the relative importance of the different mechanisms of plasmon decay can be quite different from the ones for metals. Some early works for the case of semiconductors are due to Antoncik *et al.* [15–17]. Also, there is an interesting work by Borisov *et al.* [18] about different excitations on ionic insulators.

In the following sections we regard aluminum as a free-electron gas (FEG, interacting electrons in a jellium). The two-electron wave function is expanded in a first-order Born series, the perturbing potential being an effective Yukawa electron-electron interaction. Results for the transition probability and the excitation power are presented. First and second differential spectra in both angle and energy are plotted and compared to nearly free-electron contributions as well as to binary [19] and inner-shell [20] ones. Neutralization of the incident proton is considered negligible at the velocities here considered [21,22]. We conclude that in many energy regions and directions we can tell whether an electron was excited by the decay of a plasmon or not. What is more, we can discern which plasmon process was involved.
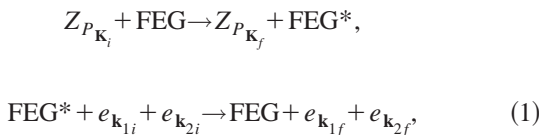
In this paper we will speak of the FEG's excitation power rather than of its stopping power. This is because we are not focusing on the projectile being "stopped " by the FEG but on electrons being excited by or via the FEG. For binary or inner shell processes it is clear that both the excitation and the stopping power per unit time will be equal. For the case of plasmons, we will speak of the stopping power in the case of plasmon creation (the projectile loses energy to create a plasmon) and of the excitation power in the case of plasmon decay (an electron is excited due to the decay of the plasmon). We regard this expressions as more precise than the ones used in I.

All nearly free electron calculations were performed for polycrystalline aluminum. Atomic units are used throughout this paper.

## II. THEORY

### A. The Hamiltonian

We are interested in the interaction of a projectile (a proton in this case) with two electrons (labeled 1 and 2), all of them embedded in a FEG. In particular, we want to study the case in which this interaction is via the excitation and decay of a plasmon in the FEG. Schematically we have

$$Z_{P_{\mathbf{K}_i}} + \text{FEG} \rightarrow Z_{P_{\mathbf{K}_f}} + \text{FEG*},$$

$$\text{FEG*} + e_{\mathbf{k}_{1i}} + e_{\mathbf{k}_{2i}} \rightarrow \text{FEG} + e_{\mathbf{k}_{1f}} + e_{\mathbf{k}_{2f}}, \tag{1}$$

where $Z_{P_{\mathbf{K}_{i,f}}}$, $e_{\mathbf{k}_{1i,f}}$, and $e_{\mathbf{k}_{2i,f}}$ are the projectile, electron 1 and electron 2 in their initial (final) states and FEG* stands for the excitation of a plasmon in the FEG.

The full Hamiltonian can be written as $H = K + V^{tot}$,

$$K = -\frac{1}{2M_P}\nabla_{\mathbf{R}}^2 - \frac{1}{2}\nabla_{\mathbf{r}_1}^2 - \frac{1}{2}\nabla_{\mathbf{r}_2}^2 - \frac{1}{2}\sum_{j\geqslant 3}\nabla_{\mathbf{r}_j}^2,$$

$$V^{tot} = V^{(P)} + V^{(e)}$$

$$= \sum_{j\geqslant 3} V_{Pj} + V_{P1} + V_{P2} + \sum_{j\geqslant 3} V_j^{(e)} + V_1^{(e)} + V_2^{(e)} + V_{12}, \tag{2}$$

where $V_{P\alpha} = -Z_P/|\mathbf{R}-\mathbf{r}_\alpha|$ is the projectile-electron Coulomb attraction ($\alpha = j,1,2$), $V_{1,2}^{(e)} = \Sigma_{j\geqslant 3}(1/|\mathbf{r}_j-\mathbf{r}_{1,2}|)$ is the interaction of electron 1 or 2 with the FEG, $V_j^{(e)} = \frac{1}{2}\Sigma'_{l\geqslant 3}V_{lj} = \frac{1}{2}\Sigma'_{l\geqslant 3}(1/|\mathbf{r}_l-\mathbf{r}_j|)$ is the total electron-electron Coulomb repulsion for electron $j$ in the FEG due to its interactions with the rest of the FEG, and $V_{12} = 1/|\mathbf{r}_2-\mathbf{r}_1|$ is the interaction of electrons 1 and 2 with each other. Coordinates $\mathbf{R}$ and $\mathbf{r}_\alpha$ represent the projectile and electron-$\alpha$ positions, respectively. Note that if the projectile is a proton, then $M_P \gg 1$.

The total potential will be approximated by

$$V^{tot} \sim V_{P1}^{eff} + V_{P2}^{eff} + V_{12}^{eff}. \tag{3}$$

In the spirit of RPA, we will define effective potentials $V_{P1}^{eff}$, $V_{P2}^{eff}$, and $V_{12}^{eff}$ that will represent interactions in the presence of the FEG. These potentials are expressed as follows ($V_{P2}^{eff}$ is not shown as it is completely analogous to $V_{P1}^{eff}$):

$$V_{P1}^{eff} = V_{P1} + \sum_{j\geqslant 3}(V_{1j}G_0^+ V_{Pj} + V_{Pj}G_0^+ V_{1j})$$

$$+ \sum_{j,l\geqslant 3, l\neq j}(V_{1l}G_0^+ V_{lj}G_0^+ V_{Pj} + V_{Pj}G_0^+ V_{lj}G_0^+ V_{1l})$$

$$+ \cdots,$$

$$V_{12}^{eff} = V_{12} + \sum_{j\geqslant 3}(V_{1j}G_0^+ V_{j2} + V_{2j}G_0^+ V_{j1})$$

$$+ \sum_{j,l\geqslant 3, l\neq j}(V_{1l}G_0^+ V_{lj}G_0^+ V_{j2} + V_{2l}G_0^+ V_{lj}G_0^+ V_{j1})$$

$$+ \cdots, \tag{4}$$

where $G_0^+ = (E-H_0+i0^+)^{-1}$ is the usual free Green operator, and each equation is a Born series for the potential considered where we have kept only those terms that can be interpreted as interactions via a number of intermediary electrons form the FEG [14].

In the case of $V_{P1}^{eff}$ and $V_{P2}^{eff}$, this expansion leads to an expression of their Fourier transforms in terms of Lindhard dielectric response. That is, $\tilde{V}_{P1}^{eff}(\mathbf{p}) = \tilde{V}_{P1}(\mathbf{p})/\varepsilon(p,\omega)$ and $\tilde{V}_{P2}^{eff}(\mathbf{p}) = \tilde{V}_{P2}(\mathbf{p})/\varepsilon(p,\omega)$ [14].

As for $V_{12}^{eff}$, its expansion is formally equal to those of $V_{P1}^{eff}$ and $V_{P2}^{eff}$, therefore it is natural to arrive at $\tilde{V}_{12}^{eff}(\mathbf{q}) = \tilde{V}_{12}(\mathbf{q})/\varepsilon(q,\omega)$. However, in order to simplify our calculations we will approximate this by the standard Yukawa potential. That is, $\tilde{V}_{12}^{eff}(\mathbf{q}) = 4\pi Z_{12}/[(2\pi)^3(q^2+\lambda^2)]$, with $\lambda = \sqrt{3}\,\omega_p/k_F$, where $\omega_p$ is the plasmon energy and $k_F$ is the Fermi velocity.

Finally, in order to allow for two-electron excitations to occur we will go beyond RPA by adding a finite width $\gamma$ to the plasmon line in Lindhard dielectric response [23]. As in I, we follow Mermin and do $\varepsilon(p,\omega)\rightarrow\varepsilon(p,\omega,\gamma)$ with $\gamma = 0.037$.

### B. Hartree wave functions

In general, the initial and final Hartree (orbital) states of the system are simply

$$\Psi_i^H = \Phi_{\mathbf{K}_i}\phi_{\mathbf{k}_{3i}}\phi_{\mathbf{k}_{4i}}\cdots F^+_{\mathbf{k}_{1i},\mathbf{k}_{2i}}\cdots,$$

$$\Psi_f^H = \Phi_{\mathbf{K}_f}\phi_{\mathbf{k}_{3f}}\phi_{\mathbf{k}_{4f}}\cdots F^-_{\mathbf{k}_{1f},\mathbf{k}_{2f}}\cdots, \qquad (5)$$

where $\Phi_{\mathbf{K}_{i,f}}$ is the projectile wave function (plane wave), $\phi_{\mathbf{k}_{ji,f}}$ is the wave function of an electron in the FEG (also a plane wave [24]), and $F^+_{\mathbf{k}_{1i},\mathbf{k}_{2i}}$ and $F^-_{\mathbf{k}_{1f},\mathbf{k}_{2f}}$ stand, respectively, for the initial and final combined wave functions of electrons 1 and 2. Both $\Phi_{\mathbf{K}_{i,f}}$ and $\phi_{\mathbf{k}_{ji,f}}$ are normalized to the Dirac $\delta$.

We will focus on the case when the FEG final state is such that $\phi_{\mathbf{k}_{3i}}=\phi_{\mathbf{k}_{3f}}$, $\phi_{\mathbf{k}_{4i}}=\phi_{\mathbf{k}_{4f}}$, etc., and $k_{ji}<k_F$ for $j\geq 3$, that is, the bulk ends in its ground state. Under these assumptions, the system's Hamiltonian can be expressed as $H=H_0+V$ with

$$H_0 = -\frac{1}{2M_p}\nabla_{\mathbf{R}}^2 - \frac{1}{2}\nabla_{\mathbf{r}_1}^2 - \frac{1}{2}\nabla_{\mathbf{r}_2}^2 + V_{12}^{eff},$$

$$V = V_{P1}^{eff} + V_{P2}^{eff}. \qquad (6)$$

Therefore we have a system composed of two interacting electrons (via the FEG) and a free projectile that is perturbed by projectile-electron interactions.

The $H_0$ eigenfunctions are the combined wave functions $F^+_{\mathbf{k}_{1i},\mathbf{k}_{2i}}$ and $F^-_{\mathbf{k}_{1f},\mathbf{k}_{2f}}$ which can be expressed as noninteracting two-electron wave functions corrected by factors $u_{i,f}^{\pm}$, that is,

$$F^+_{\mathbf{k}_{1i},\mathbf{k}_{2i}} = \phi_{\mathbf{k}_{1i}}(\mathbf{r}_1)\phi_{\mathbf{k}_{2i}}(\mathbf{r}_2)u_i^+(\mathbf{r}_2-\mathbf{r}_1),$$

$$F^-_{\mathbf{k}_{1f},\mathbf{k}_{2f}} = \phi_{\mathbf{k}_{1f}}(\mathbf{r}_1)\phi_{\mathbf{k}_{2f}}(\mathbf{r}_2)u_f^-(\mathbf{r}_2-\mathbf{r}_1), \qquad (7)$$

satisfying the two-electron Shrödinger equation

$$\left[-\frac{1}{2}\nabla_{\mathbf{r}_1}^2 - \frac{1}{2}\nabla_{\mathbf{r}_2}^2 + V_{12}^{eff} - \varepsilon_{i,f}^{1+2}\right]F^{\pm}_{\mathbf{k}_{1(i,f)},\mathbf{k}_{2(i,f)}} = 0, \qquad (8)$$

where $\varepsilon_{i,f}^{1+2}$ is the energy of the pair of electrons. Equation (8) can alternatively be expressed in a different set of coordinates [we make $\mathbf{r}=\mathbf{r}_2-\mathbf{r}_1$, $\boldsymbol{\rho}=(\mathbf{r}_1+\mathbf{r}_2)/2$, $\mathbf{k}=(\mathbf{k}_2-\mathbf{k}_1)/2$, $\boldsymbol{\kappa}=\mathbf{k}_2+\mathbf{k}_1$] as

$$\left[-\nabla_{\mathbf{r}}^2 - \frac{1}{4}\nabla_{\boldsymbol{\rho}}^2 + V_{12}^{eff} - \varepsilon_{(i,f)}\right]F^{\pm}_{\boldsymbol{\kappa}_{(i,f)},\mathbf{k}_{(i,f)}} = 0. \qquad (9)$$

The combined wave functions in this new set are

$$F^+_{\boldsymbol{\kappa}_i,\mathbf{k}_i} = \phi_{\boldsymbol{\kappa}_i}(\boldsymbol{\rho})\phi_{\mathbf{k}_i}(\mathbf{r})u_i^+(\mathbf{r}) \equiv \phi_{\boldsymbol{\kappa}_i}(\boldsymbol{\rho})\psi_{\mathbf{k}_i}^+(\mathbf{r}),$$

$$F^-_{\boldsymbol{\kappa}_f,\mathbf{k}_f} = \phi_{\boldsymbol{\kappa}_f}(\boldsymbol{\rho})\phi_{\mathbf{k}_f}(\mathbf{r})u_f^-(\mathbf{r}) \equiv \phi_{\boldsymbol{\kappa}_f}(\boldsymbol{\rho})\psi_{\mathbf{k}_f}^-(\mathbf{r}). \qquad (10)$$

We will choose this latter set of coordinates over the former as it will make the calculations in the following section much easier.

### C. The transition matrix

We build the first-order Born series for the $T$ matrix corresponding to the excitation of two electrons as

$$T^H = \langle\Psi_f^H|V_{P1}^{eff} + V_{P2}^{eff}|\Psi_i^H\rangle$$

$$= \int\int\int \Phi_{\mathbf{K}_f}^*(\mathbf{R})\phi_{\boldsymbol{\kappa}_f}^*(\boldsymbol{\rho})\psi_{\mathbf{k}_f}^{-*}(\mathbf{r})[V_{P1}^{eff}(\mathbf{r}_1-\mathbf{R})$$

$$+ V_{P2}^{eff}(\mathbf{r}_2-\mathbf{R})]\Phi_{\mathbf{K}_i}(\mathbf{R})\phi_{\boldsymbol{\kappa}_i}(\boldsymbol{\rho})\psi_{\mathbf{k}_i}^+(\mathbf{r})d\mathbf{R}d\boldsymbol{\rho}d\mathbf{r}. \qquad (11)$$

Now, expressing both potentials in terms of their Fourier transforms, making use of some previous definitions and performing some integrations we obtain

$$T^H = \tilde{V}_P^{eff}(\mathbf{p})\,\delta(\boldsymbol{\kappa}_i - \boldsymbol{\kappa}_f + \mathbf{p})\int \psi_{\mathbf{k}_f}^{-*}(\mathbf{r})$$

$$\times[e^{-i\mathbf{p}\cdot\mathbf{r}/2} + e^{i\mathbf{p}\cdot\mathbf{r}/2}]\psi_{\mathbf{k}_i}^+(\mathbf{r})d\mathbf{r}, \qquad (12)$$

where $\mathbf{p}=\mathbf{K}_i-\mathbf{K}_f$ and we have supposed that $\tilde{V}_{P1}^{eff}(\mathbf{p}) = \tilde{V}_{P2}^{eff}(\mathbf{p}) \equiv \tilde{V}_P^{eff}(\mathbf{p})$.

To the first perturbative order in $V_{12}^{eff}$, the wave function reads

$$\psi_{\mathbf{k}_i}^+(\mathbf{r}) \approx \phi_{\mathbf{k}_i}(\mathbf{r}) + g_0^+ V_{12}^{eff}(\mathbf{r})\phi_{\mathbf{k}_i}(\mathbf{r}),$$

$$\psi_f^-(\mathbf{r}) \approx \phi_{\mathbf{k}_f}(\mathbf{r}) + g_0^- V_{12}^{eff}(\mathbf{r})\phi_{\mathbf{k}_f}(\mathbf{r}), \qquad (13)$$

where $g_0^{\pm} = [k^2 + \nabla_{\mathbf{r}}^2 \pm i0^+]^{-1}$.

Again these wave functions are expressed in terms of their Fourier transforms and we get

$$\psi_{\mathbf{k}_f}^{-*}(\mathbf{r})\psi_{\mathbf{k}_i}^+(\mathbf{r}) = \frac{1}{(2\pi)^3}\int\int e^{i(\mathbf{q}-\mathbf{q}')\cdot\mathbf{r}}\left[\delta^*(\mathbf{k}_f-\mathbf{q}')\right.$$

$$+ \frac{\tilde{V}_{12}^{eff*}(\mathbf{q}'-\mathbf{k}_f)}{k_f^2-(q')^2+i0^+}\left.\right]\left[\delta(\mathbf{k}_i-\mathbf{q})\right.$$

$$+ \frac{\tilde{V}_{12}^{eff}(\mathbf{q}-\mathbf{k}_i)}{k_i^2-q^2+i0^+}\left.\right]d\mathbf{q}d\mathbf{q}'. \qquad (14)$$

If we substitute Eq. (14) into Eq. (12) keeping our calculations to zeroth order in $\tilde{V}_{12}^{eff}$, we find that one of the electrons has not made any transition and this is not the case we are interested in. So, we keep only terms of first order in $\tilde{V}_{12}^{eff}$. The final result for the transition matrix is

$$T^H = \tilde{V}_P^{eff}(\mathbf{p}) \, \delta(\boldsymbol{\kappa}_i - \boldsymbol{\kappa}_f + \mathbf{p}) \{ \tilde{V}_{12}^{eff}(\mathbf{p}_2)[g(\mathbf{k}_i, \mathbf{p}_2)$$

$$+ g(\mathbf{k}_f, -\mathbf{p}_2)] + \tilde{V}_{12}^{eff}(-\mathbf{p}_1)[g(\mathbf{k}_i, -\mathbf{p}_1) + g(\mathbf{k}_f, \mathbf{p}_1)] \},$$

(15)

where $g(\mathbf{k}, \mathbf{q}) = [k^2 - (\mathbf{k} + \mathbf{q})^2 + i0^+]^{-1}$.

### D. Hartree-Fock corrections to the wave function and transition matrix

The fact that we are dealing with two identical particles is easily added to the previous formalism. Initial and final states for the pair of electrons consist of both a spin and an orbital part. There are four possible spin states: the symmetric triplet states $(|s=1, m=\pm 1, 0\rangle)$ and the antisymmetric singlet one $(|s=0, m=0\rangle)$. The orbital part of the combined wave function must also be either totally symmetric $(F^S)$ or totally antisymmetric $(F^A)$. Therefore, instead of Eq. (10), we should write

$$(F^+_{\boldsymbol{\kappa}_i, \mathbf{k}_i})^{S/A} = \frac{\phi_{\boldsymbol{\kappa}_i}(\boldsymbol{\rho})[\psi^+_{\mathbf{k}_i}(\mathbf{r}) \pm \psi^+_{-\mathbf{k}_i}(\mathbf{r})]}{\sqrt{2}},$$

$$(F^-_{\boldsymbol{\kappa}_f, \mathbf{k}_f})^{S/A} = \frac{\phi_{\boldsymbol{\kappa}_f}(\boldsymbol{\rho})[\psi^-_{\mathbf{k}_f}(\mathbf{r}) \pm \psi^-_{-\mathbf{k}_f}(\mathbf{r})]}{\sqrt{2}}.$$

(16)

As Coulomb interactions are spin independent, the spin state for the pair of electrons remains unchanged. It follows that the symmetry of the orbital state must remain constant as well.

The Hartree-Fock transition matrix [analogous to Eq. (11)] is therefore given by

$$T^{S/A} = \langle \Psi_f^{S/A} | V_{P1}^{eff} + V_{P2}^{eff} | \Psi_i^{S/A} \rangle$$

$$= \langle s_f, m_f | s_i, m_i \rangle \langle \Phi_{\mathbf{K}_f} (F^-_{\boldsymbol{\kappa}_f, \mathbf{k}_f})^{S/A} | V |$$

$$\times (F^+_{\boldsymbol{\kappa}_i, \mathbf{k}_i})^{S/A} \Phi_{\mathbf{K}_i} \rangle,$$

$$= \delta_{s_i, s_f} \delta_{m_i, m_f} \int \int \int \Phi^*_{\mathbf{K}_f}(\mathbf{R})$$

$$\times [F^{*-}_{\boldsymbol{\kappa}_f, \mathbf{k}_f}(\boldsymbol{\rho}, \mathbf{r})]^{S/A}$$

$$\times [V_{P1}^{eff}(\mathbf{r}_1 - \mathbf{R}) + V_{P2}^{eff}(\mathbf{r}_2 - \mathbf{R})] \Phi_{\mathbf{K}i}(\mathbf{R})$$

$$\times [F^+_{\boldsymbol{\kappa}_i, \mathbf{k}_i}(\boldsymbol{\rho}, \mathbf{r})]^{S/A} d\mathbf{R} \, d\boldsymbol{\rho} \, d\mathbf{r},$$

(17)

and after some algebra the final expression for the transition matrix, analogous to Eq. (15), reads

$$T^{S/A} = \tilde{V}_P^{eff}(\mathbf{p}) \, \delta(\boldsymbol{\kappa}_i - \boldsymbol{\kappa}_f + \mathbf{p}) \{ \tilde{V}_{12}^{eff}(\mathbf{p}_2)[g(\mathbf{k}_i, \mathbf{p}_2)$$

$$+ g(\mathbf{k}_f, -\mathbf{p}_2)] + \tilde{V}_{12}^{eff}(-\mathbf{p}_1)[g(\mathbf{k}_i, -\mathbf{p}_1) + g(\mathbf{k}_f, \mathbf{p}_1)]$$

$$\pm \tilde{V}_{12}^{eff}(\mathbf{k}_{2f} - \mathbf{k}_{1i})[g(\mathbf{k}_i, -\mathbf{k}_{2f} + \mathbf{k}_{1i})$$

$$+ g(\mathbf{k}_f, -\mathbf{k}_{2f} + \mathbf{k}_{1i})] \pm \tilde{V}_{12}^{eff}(-\mathbf{k}_{1f} + \mathbf{k}_{2i})$$

$$\times [g(\mathbf{k}_i, \mathbf{k}_{1f} - \mathbf{k}_{2i}) + g(\mathbf{k}_f, \mathbf{k}_{1f} - \mathbf{k}_{2i})] \}.$$

(18)

### E. Final formula and considerations

We call binary region to the area in the $\omega$-$p$ plot where single free-electron excitations are possible. A point $(p, \omega)$ inside this region satisfies $\omega^+(p) > \omega(p) > \omega^-(p)$ $[\omega^\pm(p) = (p^2 \pm 2pk_F)/2]$ where $\mathbf{p}$ and $\omega = \mathbf{v}_i \cdot \mathbf{p}$ are the momentum and energy lost by the projectile. Note that although plasmons could be excited inside this region, they would be absorbed in the continuum of single-electron excitations and would not constitute independent modes. In order to prevent the inclusion of these pseudoplasmon processes in our results, we will keep our calculations outside the binary region.

With these considerations in mind and according to the Fermi golden rule we find that the differential probability per unit time for a given spin state $P_t(s, m)$ of two electrons being excited from $(\mathbf{k}_{1i}, \mathbf{k}_{2i})$ to $(\mathbf{k}_{1f}, \mathbf{k}_{2f})$ by a projectile that loses momentum $\mathbf{p}$ and energy $\omega = \varepsilon_{1f} + \varepsilon_{2f} - \varepsilon_{1i} - \varepsilon_{2i}$ via the excitation and decay of a plasmon is given by

$$dP_t(s, m) = 2\pi \delta(\varepsilon_{1f} + \varepsilon_{2f} - \varepsilon_{1i} - \varepsilon_{2i} - \mathbf{v}_i \cdot \mathbf{p}) |T(s, m)|^2 \Theta(k_F$$

$$- k_{1i}) \Theta(k_F - k_{2i}) \Theta(-k_F + k_{1f}) \Theta(-k_F + k_{2f})$$

$$\times \{ 1 - \Theta[\omega^+(p) - \omega(p)] \Theta[\omega(p) - \omega^-(p)] \}$$

$$\times d\mathbf{p} \, d\mathbf{k}_{1i} d\mathbf{k}_{2i} d\mathbf{k}_{1f} d\mathbf{k}_{2f}.$$

(19)

The transition matrix is symmetric for the spin singlet and antisymmetric for the spin triplet [That is, $T(0,0) = T^S, T(1,m) = T^A$]. The total probability per unit time is

$$P_t = \sum_{s=0}^{1} \sum_{m=-s}^{s} dP_t(s, m),$$

(20)

which can be written as

$$P_t = \int 2\pi \delta(\varepsilon_{1f} + \varepsilon_{2f} - \varepsilon_{1i} - \varepsilon_{2i} - \mathbf{v}_i \cdot \mathbf{p}) |T|^2$$

$$\times \Theta(k_F - k_{1i}) \Theta(k_F - k_{2i}) \Theta(-k_F + k_{1f}) \Theta(-k_F + k_{2f})$$

$$\times \{ 1 - \Theta[\omega^+(p) - \omega(p)] \Theta[\omega(p)$$

$$- \omega^-(p)] \} d\mathbf{p} \, d\mathbf{k}_{1i} d\mathbf{k}_{2i} d\mathbf{k}_{1f} d\mathbf{k}_{2f},$$

(21)

with

$$|T|^2 = |T^S|^2 + 3|T^A|^2.$$

(22)

The two electrons considered are in fact two electrons from the FEG that have been singled out. Their initial and final energies are such that $\varepsilon_{1i, 2i} < \varepsilon_F$ and $\varepsilon_{1f, 2f} > \varepsilon_F$, that is, the FEG is initially in its ground state.

### III. RESULTS

#### A. Total transition probability and excitation power

Throughout this section and the next two section, the following acronyms will be used to refer to different projectile-induced electron excitation mechanisms: NFe—plasmon de-
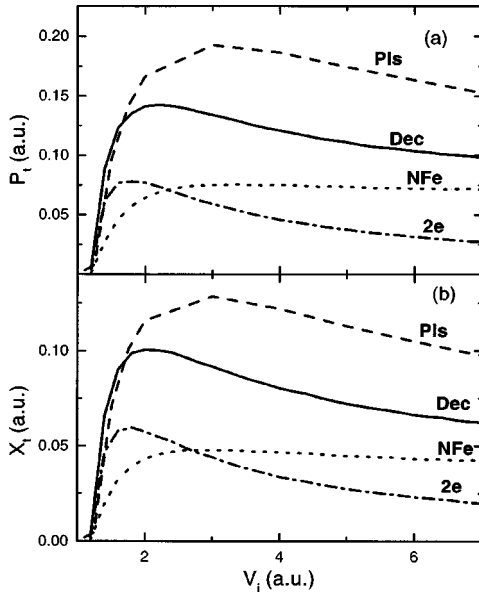
FIG. 1. (a) The total transition probability per unit time is shown for NFe and 2e contributions together with Dec=NFe+2e and the plasmon creation probability. (b) The excitation power per unit time as a function of the projectile initial velocity is shown for NFe and 2e contributions together with Dec=NFe+2e and the plasmon creation stopping power.
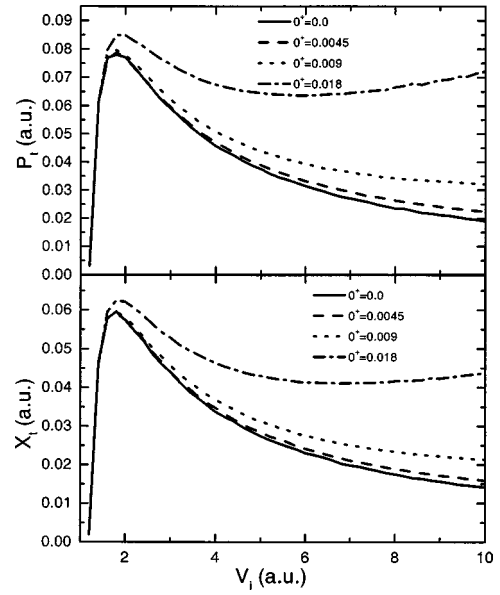


FIG. 2. The total transition probability per unit time and the excitation power per unit time as a function of the projectile initial velocity are shown for the 2e contribution considering different values for the imaginary part added to the denominators in the Green functions.

cay via the excitation of a nearly free electron. The lattice contributes with momentum associated with a site of the reciprocal lattice. Data taken from I; 2e—plasmon decay via the excitation of two interacting electrons; Bin—binary excitation of a single free electron; ISh—single inner-shell electron excitation, $1s$, $2s$, and $2p$ shell of Al were included in the calculations; Dec—Total plasmon decay (NFe+2e).

In Fig. 1(a), $P_t$ is plotted against the projectile velocity $v_i$ for NFe and 2e. Also, the sum of both contributions (Dec) is shown together with the plasmon excitation probability. It is interesting to note that Dec accounts for most of the excited plasmons (around 60% at high velocities and more than 70% for $v_i \sim 2$ a.u.) and that the inclusion of two-electron processes is important to correctly reproduce the slope of the plasmon excitation curve.

In Fig. 1(b), the excitation power per unit time is plotted against the projectile velocity. The curves shown are analogous to the ones in Fig. 1(a). Again, two-electron excitation is important to reproduce the slope of plasmon excitation. There is no energy equipartition between NFe and 2e. At high projectile velocities, the NFe contribution is dominant, while for $v_i \sim 2$ a.u. 2e is slightly greater.

However, one should not think that the relative importance of the two mechanisms considered will be the same for every metal. For a hypothetical element with the same damping as aluminum but with a larger volume per particle ($r_s = 3$ a.u. instead of the real value $r_s = 2.09$ a.u.) we found that the importance of the 2e mechanism was diminished in around 30% (considering the probability per unit time). One can conclude from this that a larger electronic density favors the 2e mechanism.

Coming back to real aluminum, the two processes combined account for most of the energy spent in the plasmon excitation; around 60% at high velocities and above 80% for $v_i \sim 2$ a.u. The question of whether plasmon excitation and decay rates were equal was put forward in I. From the previous analysis, one is inclined to think that they are in fact similar to each other. Minor contributions to the plasmon damping due to other, less important, processes, together with corrections for the two processes considered here could account for the underestimation found for the decay rates. For the case of NFe, we think contributions from fourth-order (and higher-order) neighbors in the reciprocal lattice ($\mathbf{G}_4$) could lightly improve the total results. Also, slight corrections in the potential coefficients could produce non-negligible changes in the total transition probability and excitation power. As for 2e, corrections due to exchange-correlation effects should be estimated and added to the calculations.

It is important to mention that 2e results were obtained setting the imaginary part of the Green functions in Eq. (15) equal to zero. In relation to this choice we must remark that both the transition probability and the excitation power are very sensitive to changes in this parameter. There is an implicit limit operation here to be performed after the integration. It is often the case that, for reasons of numerical convenience, a finite value is assigned to this parameter. In Fig. 2 we have plotted the transition probability and the excitation power per unit time, labeled $P_t$ and $S_t$, for two interacting electrons to be excited by the decay of a bulk plasmon as a function of the projectile initial velocity $v_i$. We considered different possible values for $0^+$ and found that not only the limit exists and is well behaved but also that we can set this parameter equal to 0 right from the start. The integrand has
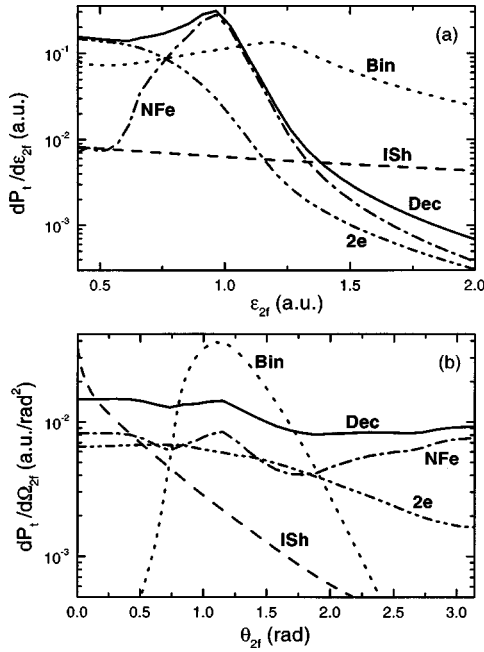
FIG. 3. (a) Single-differential transition probability as a function of electron 2 final energy (measured from the bottom of the band). (b) Single-differential transition probability as a function of $\theta_{2f}$ (electron 2 outgoing direction with respect to the projectile initial velocity). In both spectra, the projectile velocity was $V_i = 3.0$ a.u. Notation is indicated in the graph.
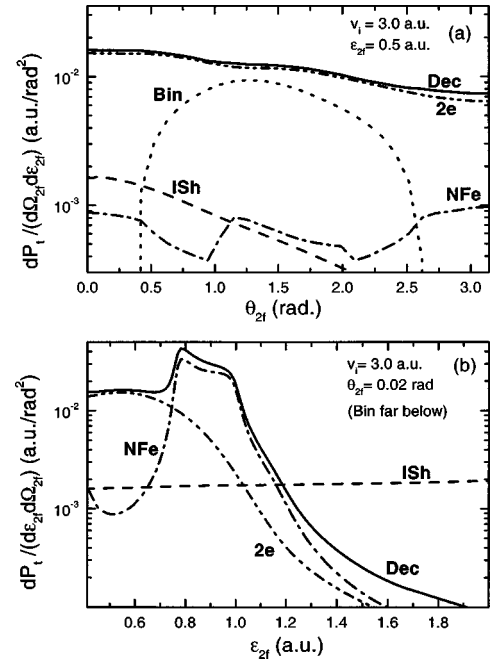


FIG. 4. (a) Double-differential transition probability as a function of $\theta_{2f}$ (excited electron outgoing direction with respect to the projectile initial velocity). Electron 2 final energy was set equal to 0.5 a.u. (b) Double-differential transition probability as a function of $\epsilon_{2f}$. The outgoing direction $\theta_{2f}$ was set equal to 0.02 rad. Notation is indicated in the graph.

no numerical complications in the region considered. Each of the denominators is forced to be nonzero because both electrons must make a transition (therefore both $\mathbf{p}_1$ and $\mathbf{p}_2$ are finite). Note also that it is only in the limit $0^+ \sim 0$ that the plasmon excitation slope is correctly reproduced.

### B. Single-differential spectra in angle and energy

We are interested in being able to tell if an electron was excited by the decay of a plasmon or by some other process. Two possible mechanisms for plasmon decay are considered: the excitation of a single nearly free electron (NFe) and the excitation of a pair of interacting electrons (2e). The energy and angular distributions for the final states of these electrons (the excited nearly free electron on one hand and electron 2, of the excited pair, on the other) are compared with those of electrons coming from nonplasmon processes such as the excitation of a single free electron (Bin) and the excitation of a single inner-shell electron (ISh). The projectile (proton) velocity was set to 3 a.u. ($v_i = 3$ a.u.). Energies are referred to the bottom of the band.

In I, we analyzed the single-differential energy spectrum for an electron excited by NFe, Bin, and ISh processes and found that around $\varepsilon_{2f} \sim 1$ a.u. NFe was the most important one. In Fig. 3(a), this energy spectra is reproduced with the addition of 2e contributions. The solid line stands for the electrons excited by plasmon decay no matter by which of the mechanisms (Dec=NFe+2e). We can see that 2e represents just a minor contribution for $\varepsilon_{2f} \sim 1$ a.u. (so the results of I remain essentially the same). However, for lower energies ($\varepsilon_{2f} \gtrsim \varepsilon_{Fer} \sim 0.41$ a.u.) it becomes the leading term to-

gether with Bin. Therefore, we conclude that electrons excited by plasmon decay concentrate in different energy regions depending on which decay process was involved.

In a completely analogous fashion, we perform the analysis of the single-differential angular spectrum shown in Fig. 3(b). The angle $\theta$ is defined relative to the projectile's direction of motion. The four processes considered are plotted together with Dec. It is clear that 2e is just a slight correction to Dec in the backward direction (so, the main result of I remains unchanged) but it is as important a contribution as NFe both in the forward and in the normal directions.

### C. Double-differential spectra in angle and energy

If we look at Fig. 3(a), it is natural to wonder how 2e and Bin compete in the low-energy region and whether it is possible to distinguish between the two processes. Therefore, we go on to analyze the second-differential angular spectrum for $\varepsilon_{2f} = 0.5$ a.u. shown in Fig. 4(a). It turns out that there are no Bin electrons either in the extreme forward or the extreme backward directions while most of 2e electrons move in the forward direction. So, we can tell if a low-energy electron comes form plasmon decay or not according to its direction of motion. Also, note that, for this energy, 2e constitutes the main contribution to Dec throughout the angular spectrum.

Likewise, Fig. 3(b) leads to the analysis of second-differential energy spectra. We consider the forward direction ($\theta_{2f} = 0.02$ radians) where 2e and ISh are the leading terms and 2e reaches its highest values. We see in Fig. 4(b) that ISh spreads quite uniformly throughout the energy range. The 2e contribution, on the other hand, is localized in the

intermediate-low energy area and for $\varepsilon_{2f} \gtrsim \varepsilon_{Fer} = 0.41$ a.u. is clearly an order of magnitude above ISh. So, in the forward direction we can tell if an electron comes from plasmon decay or not according to its energy.

## IV. SUMMARY AND CONCLUSIONS

In this paper, a simple formalism was developed to describe plasmon decay in aluminum via the excitation of two interacting electrons. The results were added to those of NFe (plasmon decay via the excitation of a nearly free electron that makes an interband transition), calculated in I, to obtain the total plasmon decay probability and excitation power. When both mechanisms for plasmon decay are considered, more than 60% of the plasmon excitation is accounted for. Also, the slope for high projectile velocities is correctly reproduced. From these results we are inclined to think that plasmon excitation and decay rates are similar to each other and that there is no other major mechanism of plasmon decay. In I, we concluded that our estimation for NFe contribution could be improved by including higher-order neighbors in the reciprocal lattice and by slight corrections in the potential coefficients. For the case of 2e contributions, we think a better wave function (for example, a Coulomb-type wave [25]) would produce higher results. Also, corrections due to exchange-correlation effects could account for some of the underestimation found.

For the case of aluminum, which was treated in this paper, it was found that for $v_i \lesssim 2$ a.u. most of the excited plasmons decay via the excitation of two interacting electrons while for $v_i \gtrsim 4$ a.u. the dominant mechanism is NFe. These results, however, should not be carelessly generalized to other metals where the relative importance of the two processes considered might not be the same. (For example, an element with a larger electronic density will favor the 2e mechanism.)

First- and second-differential spectra in angle and energy were plotted and compared to NFe ones. Nonplasmon processes such as Bin and ISh were added to the graphs in order to establish a comparison. From the analysis of these spectra we concluded that in certain energy regions and certain directions it is possible not only to identify if an electron was excited by the decay of a plasmon or not, but also to tell which plasmon-decay mechanism was involved in the excitation.

Finally, we found that most low-energy electrons traveling in the forward (with respect to the projectile initial velocity) direction had been excited by 2e mechanism for plasmon decay. Regarding this, we reckon our results combined with transport and emission estimations might explain some low energy yields found in experimental spectra for aluminum surfaces [26].

[1] D.F. DuBois, Ann. Phys. (N.Y.) **7**, 174 (1959).

[2] D.F. DuBois, Ann. Phys. (N.Y.) **8**, 24 (1959).

[3] P. Nozières and D. Pines, Phys. Rev. **113**, 1254 (1969).

[4] D.F. DuBois and M.G. Kivelson, Phys. Rev. **186**, 409 (1969).

[5] M.S. Chung and T.E. Everhart, Phys. Rev. B **15**, 4699 (1977).

[6] M. Rösler and W. Brauer, Phys. Status Solidi B **104**, 161 (1981).

[7] M. Rösler and W. Brauer, Springer Tracts Mod. Phys. **122**, 1 (1991).

[8] M. Rösler, Nucl. Instrum. Methods Phys. Res. B **90**, 537 (1994).

[9] M. Rösler, Appl. Phys. A: Mater. Sci. Process. **61**, 595 (1995).

[10] K. Sturm and L.E. Oliveira, Phys. Rev. B **24**, 3054 (1981).

[11] P.M. Platzman, E.D. Isaacs, H. Williams, P. Zschack, and G.E. Ice, Phys. Rev. B **46**, 12 943 (1992).

[12] A. Schinner, M.E. Bachlechner, and H.M. Böhm, Nucl. Instrum. Methods Phys. Res. B **93**, 181 (1994).

[13] M.E. Bachlechner, A. Holas, H.M. Böhm, and A. Schinner, Phys. Rev. B **54**, 2360 (1996).

[14] G. Bocan and J. Miraglia, Phys. Rev. A **67**, 032902 (2003).

[15] E. Antoncik, G. di Cola, and L. Farece, Radiat. Eff. **5**, 1 (1970).

[16] E. Antoncik, Radiat. Eff. **7**, 275 (1971).

[17] E. Antoncik and N.K.S. Gaur, J. Phys. C **11**, 735 (1978).

[18] A.G. Borisov, A. Mertens, H. Winter, and A.K. Kazansky, Phys. Rev. Lett. **83**, 5378 (1999).

[19] D. Arbó and J.E. Miraglia, Phys. Rev. A **58**, 2970 (1998).

[20] M.S. Gravielle (private communication).

[21] M.S. Gravielle and J.E. Miraglia, Phys. Rev. A **50**, 2425 (1994).

[22] M.S. Gravielle, Phys. Rev. A **62**, 062903 (2000).

[23] D. Mermin, Phys. Rev. B **1**, 2362 (1970).

[24] N.W. Ashcroft and N.D. Mermin, *Solid State Physics* (Holt, New York, 1976).

[25] M.S. Gravielle and J.E. Miraglia, Comput. Phys. Commun. **69**, 53 (1992).

[26] E.A. Sánchez, J.E. Gayone, M.L. Martiarena, O. Grizzi, and R.A. Baragiola, Phys. Rev. B **61**, 14 209 (2000).